BULLETIN OF
MATHEMATICAL BIOLOGY
VOLUME 38, 1976

ANALYTICAL CHARACTERIZATION OF MICROVASCULAR RESISTANCE DISTRIBUTION

H. N. MAYROVITZ and M. P. WIEDEMAN
Department of Physiology,
Temple University School of Medicine,
Philadelphia, Pennsylvania

A. NOORDERGRAAF
Department of Bioengineering,
University of Pennsylvania,
Philadelphia, Pennsylvania

The bat wing is used as an experimental preparation and as a self-contained vascular bed. The number, dimensions, and distribution of the vessels of the real vascular bed are included into an analyzable, representative geometric configuration. Based on theoretical analysis and experimental data, equations are developed and utilized to characterize the pressure-flow relationships for each branching order of the vascular field. The geometric configuration and associated describing equations are used to determine the resistance distribution of the microvascular bed. The predicted values are compared with experimentally determined quantities in normal and hypertensive animals.

Introduction. The measurement of pressure and flow in a large artery supplying a vascular bed permits the calculation of the vascular impedance to flow associated with the entire region distal to the measuring site. The low frequency limit value of the impedance is the vascular resistance and is the quantity which determines the mean value of pressure required to provide a flow sufficient to meet the needs of the dependent vascular bed being measured or studied. The derived value of vascular resistance at any instant reflects the composite properties of an array of interconnected blood vessels, and the blood within them.

For the most part previous work in modeling the microvasculature has been confined to the mesentery. The pioneering quantitative studies of Intaglietta *et al.* (1971) and Intagglietta and Zweifach (1971) have paved the way for the recent development of network models applicable to rabbit (Gross *et al.*, 1974) and cat (Lipowsky and Zweifach, 1974) mesentery vasculature. It is the intent of this communication to present the development of a first generation (prototype) microvascular characterization for purposes of predicting vascular resistance in terms of microvascular parameters in the bat wing.

The general approach is to represent the number, dimensions and distribution of vessels of a real vascular bed by a representative structural model. Each vessel of the model is then characterized by a resistance function which depends on the pressure-flow relationships applicable to that vessel. The ensemble of all such resistance functions are then used to calculate the resistance distribution throughout the bed vasculature.

Vascular Bed Structural Model. The vasculature of the wind of the small brown bat (*myotis Lucifigus*) is used as an experimental model of a self-contained vascular bed. The geometrical and dimensional data of Wiedeman (1962, 1963), as supplemented by Mayrovitz (1974) and summarized in Table I form the basis of a representative geometric configuration shown in Figure 1. All values used are average values.

Starting with the main artery at the top of Figure 1, a single pathway is illustrated in detail to the venule with the remaining pathways represented in the figure by the large arrows. Adjacent to the name of each vessel type is a number which may be termed the vessel branching "order". Each vessel illustrated in Figure 1 is further subdivided into as many axial sections as there are branches as shown in Figure 2.

Pressure–Flow Relationships

Diameter of vessel (D_i) > *undistorted cell diameter* (D_c). For those vessels which are very much larger than the red cell (i.e., main artery and artery), the pressure–flow relationship given by the Poiseuille equation is a reasonable approximation and is used in the present analysis. The general complicating factors which include the existence of the peripheral plasma layer, nonparabolic velocity profile and shear rate dependence of the effective viscosity, do not appear significantly to alter the resistance function provided that the appropriate value of viscosity is used in the Poiseuille equation.

The situation in the small artery and venule is more complicated in that the flow region lies between the single cell capillary case and the "continuum" main

artery case. In the venous vessels, there is the further complication associated with the existence of an effective yield stress, which becomes increasingly important as the shear rate becomes lower. The significance of these factors with respect to the calculation of bed input resistance is negligible (Mayrovitz, 1974) and may be neglected in the normal state.

The flow regime and, more specifically, the resistance functions of these vessels is represented in a fashion similar to the larger vessels (Noordergraaf, 1969). Using the subscript i to denote vessel branching order, each of the m_i

TABLE I

Vessel Diameters, Lengths, and Average Number of Branches used to Construct Structural Model

Vessel	Diameter (Microns)	Length (mm)	Number of Branches
Main artery	97.0	40.0	13.0
Artery	52.0	17.0	12.0
Small artery	19.0	3.5	9.7
Arteriole	7.0	0.95	4.6
Terminal arteriole	5.0	0.20	3.1
Capillary	3.7	0.23	—
Post capillary venule	7.3	0.21	—
Venule	21.0	1.0	5.0
Small vein	37.0	3.4	14.1
Vein	76.0	17.6	24.5

axial segments representing the vessels (Figure 2) having length l_i, diameter D_i, and blood viscosity η_b, has a resistance given by

$$r_i = \frac{128\eta_b l_i}{m_i \pi D_i^4} . \tag{1}$$

Diameter of vessel $\leqslant$ undistorted red cell dimension. The fluid dynamics of the arteriole, terminal arteriole, capillary and post capillary venule having a mean diameter range from 3.7 to 7 μm are developed on the basis of single file erythrocyte flow. The resistance function is developed along the following lines. We consider n cells distributed in an ith order vessel having total length l_i and inside diameter D_i.

The pressure drop in the plasma region between adjacent cells for a given mean flow deviates from that given by the Poiseuille relationship (1) due to the flow field modification in the vicinity of the cells leading surface, and due to the

presence of the downstream cell and its alteration of the boundary conditions by its presence. The influence of a single cell is approximated in the present analysis by utilizing and extending the results obtained by Barnard (1969), who treated the cell as a freely deformable surface and solved the resulting nonlinear boundary value problem numerically via successive iterations. By

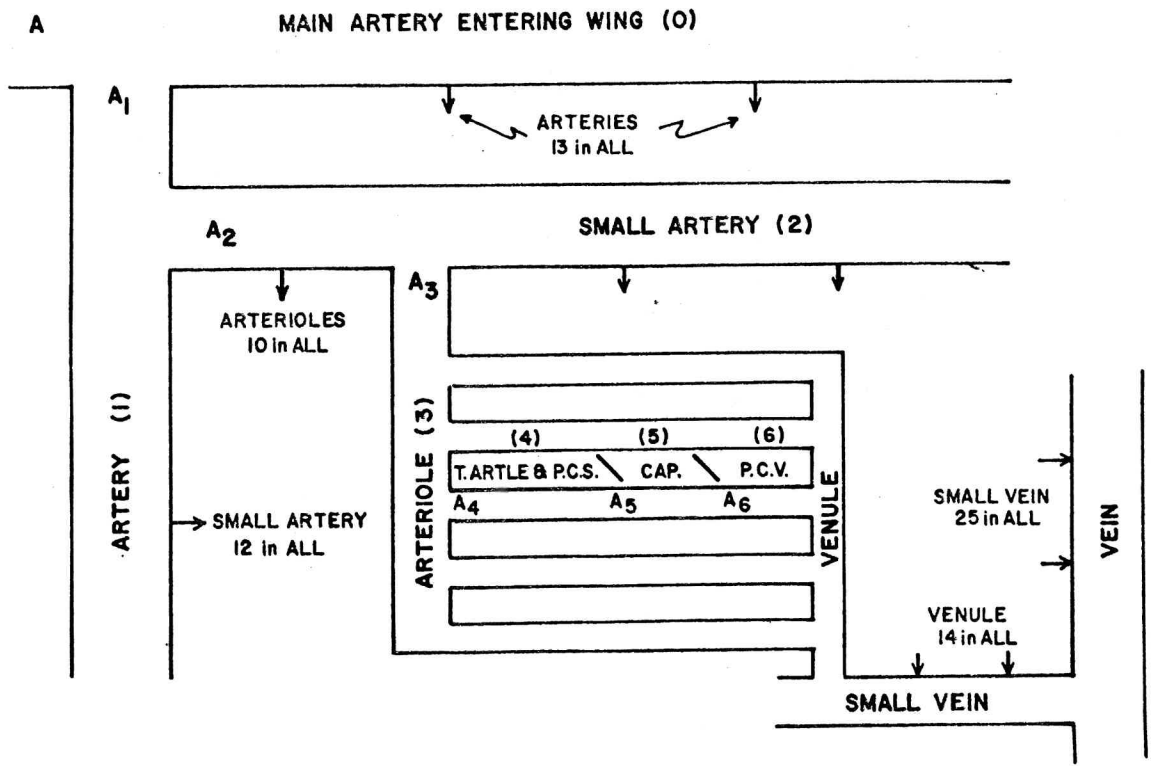

Figure 1. Topological Model. One pathway from main artery to small vein is shown in detail and the remainder of the branches and vascular pathways are shown as straight arrows. Each vessel is given a name in accordance with those put forward by Wiedeman (1962) and in addition a branching order designation is shown in parenthesis. The A's are used for reference to denote particular arteriolar sites. Dimensions and branching distribution are as given in Table 1. T. Artle = terminal arteriole, P.C.S. = precapillary sphincter, CAP = capillary, P.C.V. = post capillary venule

curve-fitting we have represented the numerical solutions obtained for the three-dimensional case in closed form (2 and 3 below).

We introduce the following definitions:

$\frac{\Delta P}{\Delta X_1}$ = mean pressure gradient across the cell

η = plasma viscosity

u_c = red cell velocity

u_p = mean plasma velocity
D_i = inside diameter of vessel
D_c = undistorted cell dimension
$v = D_c/D_i$
k = a constant = 1.14
l_c = effective axial length of red blood cell
l_p = effective axial length of plasma gap
l_i = length of vessel.

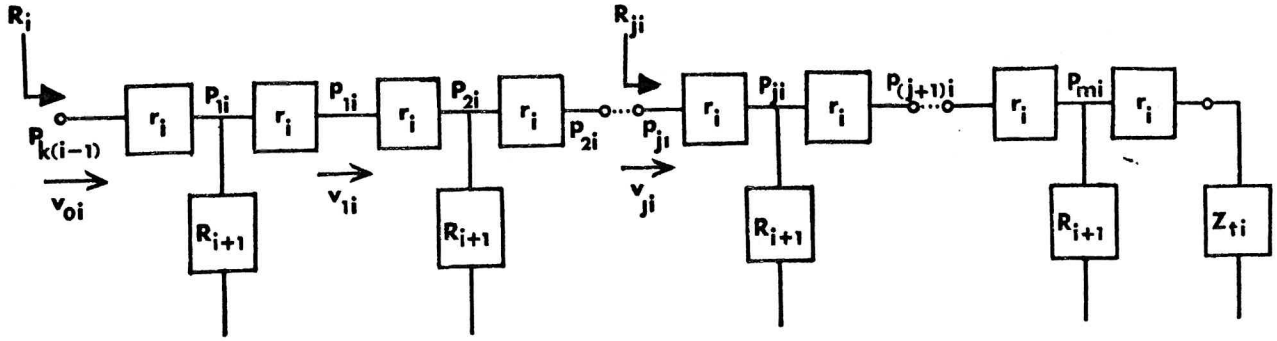

Figure 2. Detailed representation of vessels. Each vessel of the structural model is represented by as many "T" sections as there are branches. This figure illustrates the general relationships for an i^{th} order vessel. For example, if $i = 2$, r_i represents the longitudinal resistance of the small artery (2nd order branch) and R_{i+1} the total resistance looking toward the capillary at each of the branching sites of the small artery, i.e., looking into the arteriole. The pressure at the origin, $P_{j(i-1)}$, is the pressure at the j^{th} branch of the $(i-1)$ vessel (artery) and the pressure P_{ji} serves as the input pressure for the $(i+1)$ order vessels. The quantities R_{ji}, p_{ji} and v_{ji} denote mean resistance, pressure and velocity at the j^{th} segment of the i^{th} order vessel. The quantity R_i is the total resistance seen looking into the i^{th} order vessel at its origin

The fundamental quantitative relationships for a single cell are the following:

$$\frac{\Delta P}{\Delta X_1} = \frac{16\eta u_c}{D_i^2}\left[1 + \left(\frac{v}{4}\right) + \left(\frac{v}{4}\right)^4\right] \tag{2}$$

$$u_c = (2 - e^{-k/v})u_p \tag{3}$$

The effect of a finite separation of cells is approximated using the numerical solution due to Lew and Fung (1970), from which we develop the closed form characterization (4) below. Strictly speaking, effects within the plasma region for the idealized red cell shape analyzed by Lew and Fung depend on both cell separation and intravascular red cell dimension to vessel diameter. For a given cell separation and mean flow, the plasma region pressure gradient increases

with increasing ratio of D_c/D_i. The maximum value of this ratio is unity and would constitute true plug flow. For this case, the mean pressure gradient in a plasma region of length ΔX_2 may be expressed as:

$$\frac{\Delta P}{\Delta X_2} = \frac{32\eta u_2}{\pi D_i^2}(1+0.6\,e^{-\beta}) \tag{4}$$

in which:

β = cell separation expressed in vessel diameters.

The total pressure drop across the length of the vessel is taken as the sum of the individual pressure drops. Using (2) through (4) the total pressure drop across a vessel having n cells (ΔP_T) is then given by

$$\Delta P_T = \frac{128\eta Q}{\pi D_i^4}\left\{(2-e^{-k/\nu})\left[1+\left(\frac{\nu}{4}\right)+\left(\frac{\nu}{4}\right)^4\right]\frac{l_c}{2}+(1+0.6\,e^{-\beta})l_p\right\}n, \tag{5}$$

in which

$$Q = \pi D_i^2 u_p/4,$$

and the form of the resistance function for each of the axial segments of Figure 2 in which $\nu \geqslant 1$ are given by (6)

$$r_i = n\frac{64\eta}{\pi m_i D_i^4}\left\{(2-e^{-k/\nu})\left[1+\left(\frac{\nu}{4}\right)+\left(\frac{\nu}{4}\right)^4\right]\frac{l_c}{2}+(1+0.6\beta)l_p\right\}. \tag{6}$$

Resistance Distribution. Each of the vessels shown in Figure 1 is characterized in accordance with the detailed representation of Figure 2. The hydraulic resistances of the axial segments for each vessel have values defined by (1) or (6) depending on their diameter to RBC ratio. The shunt resistances at each branch point have values equal to the total input resistance seen looking toward the capillary at each of the m_i branching sites.

We introduce the following definitions:

$\gamma_i = \cosh^{-1}\left(1+\frac{r_i}{R_i+1}\right)$ = propagation constant of an i^{th} vessel order

$Z_{ci} = r_i(r_i+2R_{i+1})$ = characteristic impedance of an i^{th} order vessel

Z_{ti} = terminating impedance of the m^{th} segment of an i^{th} order vessel

$\rho_i = \frac{Z_{ci}}{Z_{ti}}$ = ratio of characteristic to terminating impedance

R_i = total input resistance seen looking into an i^{th} order vessel at its origin.

We then have

$$R_i = Z_{ci}\left\{\frac{\rho_i \sinh m_i\gamma_i + \cosh m_i\gamma_i}{\sinh m_i\gamma_i + \rho_i \cosh m_i\gamma_i}\right\}, \qquad i = 0, 1, 2. \quad (7)$$

Equation (7) is the hemodynamic analog (Noordergraaf, 1969) of the classical electrical network theory equation and is used to determine the total input resistance seen looking into a branch from its parent vessel (e.g. as illustrated by sites A_1, A_2, etc. in Figure 1). As written, (7) is sufficiently general so as to account for vessel impedances. The resistance function specification of each vessel segment in the present analysis implies that both characteristic impedance and terminating impedance (and hence their ratio, ρ) are real functions. Pulsatile aspects of the hemodynamics and compliance effects (Gross *et al.*, 1974) as they relate to the bat wing microcirculation are dealt with elsewhere (Mayrovitz *et al.*, 1975a).

Result and Comparison with Experimental Data

Normal vasculature. Using the model equations, input resistances for the five arterial branching orders were determined.

To evaluate the accuracy of the model predictions the resistance at the first order branching level was determined experimentally and estimated from the data of Wells (1971). Technical difficulties preclude measurements at other levels.

The main artery of the wing was cannulated in a retrograde fashion in a manner previously reported (Wiedeman, 1968). The cannula was filled with buffered saline and connected via a *t*-tube to a low compliance pressure transducer (Microdot MS). Using a syringe the stagnant column of saline in the cannula was advanced to a point just distal to a branch of the cannulated vessel. The pressure measured under these conditions was taken as the pressure at the origin of the first order branch. The stagnant saline column was then advanced slightly so that a small bolus of saline was caused to enter the first order branch. Using a photoptic system, the transit time of the bolus between two axially separated sites along the vessel was measured and used to calculate average velocity. Vessel diameters were measured using a calibrated eyepiece micrometer and average flow calculated as the product of average velocity and cross-

sectional area. The resistance seen looking into the first order branch was then calculated as the ratio of pressure to flow. A total of 13 measurements were made in four animals.

Table II summarizes the comparisons between predicted resistance values and those calculated from experimental data. The experimental results represent the mean value of the 13 separate resistance calculations. The standard deviation of the first order resistance was 0.4×10^9 dynes cm^{-5} sec. Note that the input resistances (i.e. the equivalent driving point resistance) for a given vessel type increases as the capillary is approached from the arterial side. The close agreement between the predicted and measured values of first order input resistances supports the appropriateness of the model employed as a useful predictor for the normal vasculature.

TABLE II

Summary of Predicted Resistance Values and Those Calculated from Experimental Data. R_i is the Input Resistance at the i^{th} Branching Order. Measured Data Available for First Order Branching Level Only

	R_i (dynes cm^{-5} sec)		
	Predicted	Experimental	
Branching order		Present work	Wells (1971)
0	5.03×10^8		
1	3.74×10^9	3.6×10^9	3.4×10^9
2	2.88×10^{10}		
3	1.77×10^{11}		
4	6.81×10^{11}		

Hypertensive vasculature. A recent report on the changes in vascular morphology concomitant with deoxycorticosterone acetate induced hypertension (Friedman *et al.*, 1971) provided additional experimental data from which the predictive value of the model may be further evaluated. The data consist of the radii, muscle cell morphology and vessel wall area measured using a quick-freezing technique in the superficial epigastric artery and arteriole in control and hypertensive rats. Measurement of pressure in the tail artery showed the existence of two hypertensive groups classified as low, or intermediate hypertensive (H_L) and high hypertensive (H_H). We want to determine whether the model would predict the measured changes in blood pressure when the morphological changes of the vessels of the hypertensive animal were appropriately incorporated into the model. To test this, Friedman's data was used to calculate the percentage change in vascular diameter in artery and arteriole. Using the

structure of Figure 1 as a reference vascular bed, and its input resistance as a reference resistance ($R^{(0)}_{\text{reference}}$) the hypertensive vascular diameter changes were incorporated into the model and "hypertensive" resistances ($R^{(0)}_H$) calculated for the high and low hypertensive groups. The results obtained are shown in Table III.

In the first column of Table III, the model, with characteristics given by Table I is used to represent the vascular state of Friedman's experimental control group, and the increase in resistance associated with the low hypertensive group is expressed as a resistance increase factor defined as $R^{(0)}_H/R^{(0)}_{\text{reference}}$. The resistance factor predicts an increase in mean pressure (assuming no flow

TABLE III

Comparison of Measured and Predicted Hypertensive Changes

	Control Group (reference) compared with Group L	Group L (reference) compared with Group H
$R_{\text{reference}}{}^{(0)}$	5.02	5.02
$R_H{}^{(0)}$	6.96	6.89
Predicted resistance increase factor	1.38	1.37
Measured mean blood Pressure increase factor	1.13	1.31

$R_{\text{reference}}{}^{(0)}$ is the input resistance as calculated from the topological model. $R_H{}^{(0)}$ is the input resistance calculated from the topological model with vessel diameter changes simulating those observed by Friedman. Resistance increase factor is the ratio $R_H{}^{(0)}/R_{\text{reference}}{}^{(0)}$. Mean pressure increase factor is the measured ratio of hypertensive mean pressure to a reference mean pressure. Resistances are in units of 10^8 dynes cm^{-5} sec.

change) by a factor of 1.38. The measured increase is only 1.13. In the second column, the vascular model is used to represent the vascular state of the low hypertensive group, and the incerase in resistance of the high hypertensive group is expressed as the resistance increase factor. The agreement between the model prediction with respect to the mean pressure in the high hypertensive group in this case is better (1.37 vs. 1.31). In each case the model predicts a higher mean pressure than was actually measured.

Discussion. In this paper a first generation model of the vasculature of the bat wing has been developed. It has been shown that given sufficient information about the architecture and metrics it is feasible to develop a microvascular representation using theoretical fluid dynamic formulations. The specific aspect with which the bulk of this paper is concerned is the prediction of the vascular

bed resistance. This, the model did quite well. From several points of view the model is not excessively complex. It does not deal in impedance, but rather resistance. A number of the complicating rheologic factors are not yet included and the post capillary vasculature has not yet been included in any extensive fashion. Yet, the model predictions were within a few percent of the measured values obtained by the author, and as calculated from limited data available in the literature.

As it is presently formulated, the model is strictly applicable to the bat wing. The potential utility as well as the hazards associated with extrapolating to other vasculatures is well illustrated by testing the applicability of the wing vasculature as a model to predict hypertensive pressure changes. Perfect agreement between the predicted and measured pressure rise corresponding to the two hypertensive subgroups would mean (1) that the vessel dimensional changes measured on a sample basis are characteristic of all vessel changes; (2) that the model topology and structure adequately represent the essential characteristics of the entire vascular system with respect to bed resistance, and (3) other changes in vascular of hemodynamic characteristics are negligible with respect to their effect on bed resistance. That the perfect agreement is not achieved is not surprising in view of the several difficulties in extrapolating the hypertensive data. The measured data distinguish between two vessel types, whereas the vascular model consists of five vessel orders on the arterial side. Thus, it is necessary to assign radius reduction factors according to some criteria developed for the purpose. In the results that are presented here, the main artery radius changes were programmed to correspond to the epigastric artery changes and the other vessel orders to the arteriole hypertensive changes. Assuming that this is an adequate description of changes within the vascular region measured, there is no direct evidence that these changes are representative of changes within the remaining vascular beds. If we assume that they are representative, then the differences in the relative contribution to total resistance of each bed must be considered. In the present analysis, the predicted pressure increase is based on a uniform contribution and is probably a major reason why the pressure increase is larger than that measured. Another factor is the effect of possible changes in cardiac output on the measured pressure. Cardiac output was not measured, but small reductions in the hypertensive groups would have the tendency to bring the predicted values closer to the measured values of pressure. The fact that the predictive quality of the model was best when the comparison was made between the low and the high hypertensive group could indicate that there were differences other than dimensional between the control and hypertensive groups, but that because these were differences common to both hypertensive groups they were less significant with respect to the pressure comparison.

The inadequacy of the hypertension prediction notwithstanding, the microvascular representation developed and utilized represents an initial and basic framework for microvascular characterization. It is a characterization method applicable to other vascular beds providing that appropriate specific refinements are incorporated. An advantage of the representation used is that the effects of changes in diameter of individual vessel orders (vasomotion) as they relate to changes in vascular bed resistance and microcirculation hemodynamics may be incorporated and evaluated (Mayrovitz *et al.*, 1975b). Thus, it provides the required framework for incorporating non-uniform systems and local control acting on the several vessel orders and evaluating the composite and separate significances of these controls on changing vascular resistance. This control represents a parametric change of the diameter and physical properties of identifiable vessels which in turn alter vascular bed resistance and microvascular resistance distribution. Such controls have not been implicitly incorporated here, because it was our purpose to develop a first generation model of the system to be controlled and because of the lack of quantitative information concerning the characteristics of this parametric control. However, by utilizing the basic representative approach developed here, a foundation for a more comprehensive microvascular characterization of specific vascular regions of the body is now available. Further, by modifying the basic vessel segment representation to include frequency–dependent parameters, it is possible to use the geometrical configuration structure to determine the input impedance at the several branching order levels as a function of frequency, i.e. $Z_{\text{in}}(w)$.

This work was supported in part by NHLI grant No. HL 142 17.

LITERATURE

Barnard, A. C., L. Lopez and J. D. Hellums. 1969. "Basic Theory of Blood Flow in Capillaries." *Microvas. Res.*, **1**, 23–34.

Friedman, S. M., M. Nakashima and M. A. Mar. 1971. "Morphological Assessment of Vasoconstriction and Vascular Hypertrophy in Sustained Hypertension in the Rat." *Microvas. Res.*, **3**, 416–425.

Gross, J. F., M. Intaglietta and B. W. Zweifach. 1973. "Network Model of Pulsatile Hemodynamics in the Microcirculation of the Rabbit Omentum." *Am. J. Physiol.*, **226**, 1117–1123.

Intaglietta, M., D. R. Richardson and W. R. Tompkins. 1971. "Blood Pressure, Flow, and Elastic Properties in Microvessels of Cat Omentum." *Am. J. Physiol.*, **221**, 922–927.

——— and B. W. Zweifach. 1971. "Geometrical Model of the Microvasculature of Rabbit Omentum from In Vivo Measurements." *Circ. Res.*, **28**, 593–600.

Lew, H. S. and Y. C. Fung. 1970. "Plug Effect of Erythrocytes in Capillary Blood Vessels." *Biophys. J.*, **10**, 80–91.

Lipowsky, H. H. and B. W. Zweifach. 1974. "Network Analysis of Microcirculation of Cat Mesentery." *Microvas. Res.*, **7**, 73–83.

Mayrovitz, H. N. 1974. "The Microcirculation: Theory and Experiment," Ph.D. Dissertation, University of Pennsylvania.

———, M. P. Wiedeman and A. Noordergraaf. 1975a. "Interaction in the Microcirculation." In: *Cardiovascular System Dynamics,* MIT Press (in press).

———, ——— and ——— 1975b. "Microvascular Hemodynamic Variations Accompanying Microvessel Dimensional Changes." *Microvas. Res.* (in press).

Noordergraaf, A. 1969. Hemodynamics. In: *Biological Engineering,* Ed. Schwan, H. P., pp. 391–545. New York: McGraw-Hill Book Company.

Wells, L. A. 1971. "Circulatory Patterns of Hibernators." *Am. J. Physiol.,* **221,** 1517–1523.

Wiedeman, M. P. 1968. "Blood Flow through Terminal Arterial Vessels after Denervation of the Bat Wing." *Circ. Res.,* **22,** 83–89.

———. 1962. "Lengths and Diameters of Peripheral Arterial Vessels in the Living Animal." *Circ. Res.,* **10,** 686–690.

———. 1963. "Dimensions of Blood Vessels from Distributing Artery to Collecting Vein." *Circ. Res.,* **12,** 375–381.

RECEIVED 9-9-75
REVISED 7-27-75